

1 **Revision 1**

2 **Controls on tetrahedral Fe(III) abundance in 2:1 phyllosilicates - - Discussion**

3 PETIT SABINE\*, BARON FABIEN, AND DECARREAU ALAIN

4 Institut de Chimie des Milieux et Matériaux de Poitiers (IC2MP), UMR 7285 CNRS, Université de  
5 Poitiers, F-86073 Poitiers Cedex 9, France

6

7

8 Corresponding Author:

9 Sabine PETIT

10 Present address:

11 UMR 7285 CNRS, Université de Poitiers, F-86073 Poitiers Cedex 9, France.

12 \*E-mail: [sabine.petit@univ-poitiers.fr](mailto:sabine.petit@univ-poitiers.fr)

13

14

15

16 **ABSTRACT**

17 Cuadros et al. (2019) used a wide range of data from dioctahedral and trioctahedral Fe<sup>3+</sup>-bearing  
18 2:1 phyllosilicates, to propose a model describing how tetrahedral occupancy by Fe<sup>3+</sup> takes place  
19 in both dioctahedral and trioctahedral 2:1 phyllosilicates. The partition coefficient approach  
20 (Decarreau and Petit, 2014) while focusing on distribution of Al<sup>3+</sup> and Fe<sup>3+</sup> between octahedral  
21 and tetrahedral sites of dioctahedral smectites has been disregarded in the Cuadros et al. (2019)'s  
22 study. This approach was applied here on the Cuadros et al. (2019)'s set of data. The partition  
23 coefficient value linked to the distribution of Al<sup>3+</sup> and Fe<sup>3+</sup> between octahedral and tetrahedral  
24 sites determined from natural and synthetic dioctahedral smectites applies well to trioctahedral  
25 phyllosilicates too. Data from synthetic iron-rich 2:1 smectites fit also well with both Cuadros et  
26 al. (2019) and Decarreau and Petit (2014) models.

27

28 **Keywords:** 2:1 phyllosilicates, tetrahedral Fe, partition coefficient, smectite, nontronite.

29

30  
31  
32 Cuadros et al. (2019) used a wide range of data (70 samples) concerning dioctahedral and  
33 trioctahedral Fe<sup>3+</sup>-bearing 2:1 phyllosilicates, to propose a model describing how tetrahedral  
34 occupancy by Fe<sup>3+</sup> takes place in both dioctahedral and trioctahedral 2:1 phyllosilicates. The data  
35 came from the investigation of 2:1 phyllosilicates of submarine hydrothermal origin (29) and  
36 from literature (41).

37 Cuadros et al. (2019) wrote: “With respect to *cation competition* for specific sites in  
38 phyllosilicates, it appears that the radius and charge of Si<sup>4+</sup>, Al<sup>3+</sup>, Fe<sup>3+</sup>, Fe<sup>2+</sup>, and Mg<sup>2+</sup> only allow  
39 Al<sup>3+</sup> and Fe<sup>3+</sup> to occupy both tetrahedral and octahedral sites. The relative stability of these two  
40 cations in the two sites should be a control for Fe(III) distribution between both sites”. On the  
41 basis of this largely accepted assumption, and using the formalism for intra-crystalline  
42 homovalent ions exchange between two nonequivalent sites, Decarreau and Petit (2014) proposed  
43 a preexisting model based on a partition coefficient approach contradicting Cuadros et al.  
44 (2019)’s claim to report for the first time a model of Fe<sup>3+</sup> distribution in 2:1 phyllosilicates.  
45 Decarreau and Petit (2014) showed that the distribution of Al<sup>3+</sup> and Fe<sup>3+</sup> between octahedral and  
46 tetrahedral sites of dioctahedral smectites was controlled by a partition coefficient  $K_{d(4/6)} =$   
47  $[\text{Fe}^{3+}_4 * \text{Al}^{3+}_6] / [\text{Fe}^{3+}_6 * \text{Al}^{3+}_4]$ , ( $\text{Fe}^{3+}_4 = \text{Fe}^{3+} / (\text{Fe}^{3+} + \text{Al}^{3+})$ ) molar ratio in tetrahedra, 4 and 6  
48 referring to tetrahedral and octahedral sites; similar relations for Al<sup>3+</sup>), and a  $K_{d(4/6)}$  value of  
49 0.006 was obtained from the fit of data from natural smectites formed at low temperature. This  
50 very low  $K_{d(4/6)}$  value was consistent with the physical model of Brice (1975), widely used for  
51 the partitioning of elements in geochemistry. The model of Brice (1975) also predicts an increase  
52 in  $K_{d(4/6)}$  with the increase of temperature of mineral formation. Accordingly, a  $K_{d(4/6)}$  value of  
53 0.02 was measured from synthesis experiments of dioctahedral smectites at 200°C (Decarreau

54 and Petit, 2014). All data of Cuadros et al. (2019) (supplementary file S1) were plotted on a  
55 classical geochemical diagram ( $\text{Fe}^{3+}_4$  vs  $\text{Fe}^{3+}_6$ ) to evaluate a Kd value (Fig. 1). Most of the data  
56 are consistent with  $\text{Kd}_{(4/6)}$  values ranging from 0.006 to 0.02 except two trioctahedral samples  
57 (ferriphlogopite with no  $\text{Al}^{3+}_6$  and talc/smectite with almost no  $\text{Fe}^{3+}_6$  and  $\text{Al}^{3+}_6$ ) and three  
58 nontronites (HQ and two NG1 with different structural formulae). The partition coefficient  
59 approach of Decarreau and Petit (2014), established for dioctahedral smectites, appears efficient  
60 for a large variety of both di- and tri-octahedral 2:1 phyllosilicates. A single  $\text{Kd}_{(4/6)}$  value suits to  
61 most samples irrespective of their di- or tri-octahedral character and of their amount of  $\text{M}^{2+}$   
62 (Fig.1).

63 It is possible to evaluate the amount of tetrahedral  $\text{Fe}^{3+}$  from the total amount of  $\text{Fe}^{3+}$  and the  
64  $\text{Kd}_{(4/6)}$  value determined by Decarreau and Petit (2014), fixing the amount of octahedral  $\text{M}^{2+}$   
65 cations and the layer charge. The Cuadros et al (2019)'s data of figure 1 were reported on figure  
66 2. Most of di- and tri-octahedral samples fit well using a  $\text{Kd}_{(4/6)}$  value of 0.006, a tetrahedral  
67 charge of 1, and an amount of  $\text{M}^{2+}$  cations from 0.2 to 0.8 (for  $\text{O}_{20}(\text{OH})_4$ ) (Fig.2). The  
68 trioctahedral samples that are out of the range are micas and Fe-rich saponites with none or very-  
69 low total amount of Al. Nevertheless, the data are consistent with a low  $\text{Kd}_{(4/6)}$  value (Fig.2).

70 For the selection of literature data, Cuadros et al. (2019) disregarded some relevant data  
71 concerning micas (Semenova et al., 1984) and excluded some data from synthetic nontronites  
72 (Petit et al., 2015; Baron et al., 2016) because tetrahedral  $\text{Fe}^{3+}$  was mainly obtained using IR  
73 spectroscopy. Due to their high total  $\text{Fe}^{3+}$  and high  $\text{Fe}^{3+}_4$  amounts compared to natural samples,  
74 the series of well characterized synthetic nontronites are interesting samples to study iron status  
75 in clay minerals (Petit et al., 2017). Several studies gave strong evidence that the wavenumber of  
76 several IR bands, and notably the main Si-O band at about  $1000\text{ cm}^{-1}$  can be used efficiently to  
77 quantify the octahedral and tetrahedral  $\text{Fe}^{3+}$  amounts (Petit et al., 2015; Baron et al., 2016). These

78 samples of Baron et al. (2016) were also studied by chemical analysis using scanning electron  
79 microscope equipped with an energy dispersive spectrometer, Mössbauer spectroscopy (Baron et  
80 al., 2017), and by X-ray diffraction that supported well the IR results. Cuadros et al. (2019)  
81 alleged that these data from synthetic nontronites fit their regression. Why thus exclude these data  
82 for their study?

83

84

## REFERENCES

85

86 Baron, F., Petit, S., Tertre, E., and Decarreau, A. (2016) Influence of aqueous Si and Fe  
87 speciation on tetrahedral Fe (III) substitutions in nontronites: a clay synthesis approach. *Clays  
88 and Clay Minerals*, 64, 230–244.

89 Baron, F., Petit, S., Pentrák, M., Decarreau, A., and Stucki, J. W. (2017) Revisiting the nontronite  
90 Mössbauer spectra. *American Mineralogist*, 102, 1501–1515.

91 Brice J.C. (1975) Some thermodynamic aspects of the growth of strained crystals. *Journal of  
92 Crystal Growth*, 28, 249-283.

93

94 Cuadros, J., Michalski, J. R., Darby Dyar, M., and Dekov, V. (2019) Controls on tetrahedral Fe  
95 (III) abundance in 2:1 phyllosilicates. *American Mineralogist*, 104, 1608–1619.

96

97 Decarreau, A., and Petit, S. (2014) Fe<sup>3+</sup>/Al<sup>3+</sup> partitioning between tetrahedral and octahedral sites  
98 in dioctahedral smectites. *Clay Minerals*, 49, 657-665.

99

100 Petit, S., Decarreau, A., Gates, W., Andrieux, P., and Grauby, O. (2015) Hydrothermal synthesis  
101 of dioctahedral smectites: The Al-Fe<sup>3+</sup> chemical series. Part II: Crystal-chemistry. *Applied Clay  
102 Science*, 104, 96–105.

103

104 Petit, S., Baron, F., and Decarreau, A. (2017) Synthesis of nontronite and other Fe-rich smectites:  
105 a critical review. *Clay Minerals*, 52, 469–483.

106

107 Semenova, T.F., Rozhdestvenskaya, I.V., and Frank-Kamenetskii, V.A. (1984) The structural  
108 characteristics of micas with tetrahedral iron content regarding isomorphous substitutions. *Acta  
109 Crystallographica*, A40, C257-C258.

110

111

112

## Figure captions

113

114 **Figure 1:** Plot of  $\text{Fe}^{3+}_4$  vs  $\text{Fe}^{3+}_6$  molar ratio (see text). Squares: dioctahedral phyllosilicates;  
115 triangles: trioctahedral phyllosilicates. Open symbols: outlying data (see text). Red curve:  $\text{Fe}^{3+}_4$   
116 vs  $\text{Fe}^{3+}_6$  values in the case of a partition coefficient  $\text{Kd}_{(4/6)} = 0.006$ ; green curve:  $\text{Fe}^{3+}_4$  vs  $\text{Fe}^{3+}_6$   
117 values in the case of a partition coefficient  $\text{Kd}_{(4/6)} = 0.02$ .

118  
119 **Figure 2:** Plot of  $\text{Fe}^{3+}_4$  vs total  $\text{Fe}^{3+}$  (for  $\text{O}_{20}(\text{OH})_4$ ). Squares: dioctahedral phyllosilicates;  
120 triangles: trioctahedral phyllosilicates. Open symbols: outlying data (dioctahedral data in Fig. 1);  
121 Curves were calculated with  $\text{Kd}_{(4/6)} = 0.006$ . Blue curve:  $\text{M}^{2+} = 0.2$  and tetrahedral charge = 1;  
122 green curve:  $\text{M}^{2+} = 0.8$  and tetrahedral charge = 1; violet curve:  $\text{M}^{2+} = 3$  and tetrahedral charge =  
123 1; red curve:  $\text{M}^{2+} = 3.85$  and tetrahedral charge = 2.

124

Figure 1

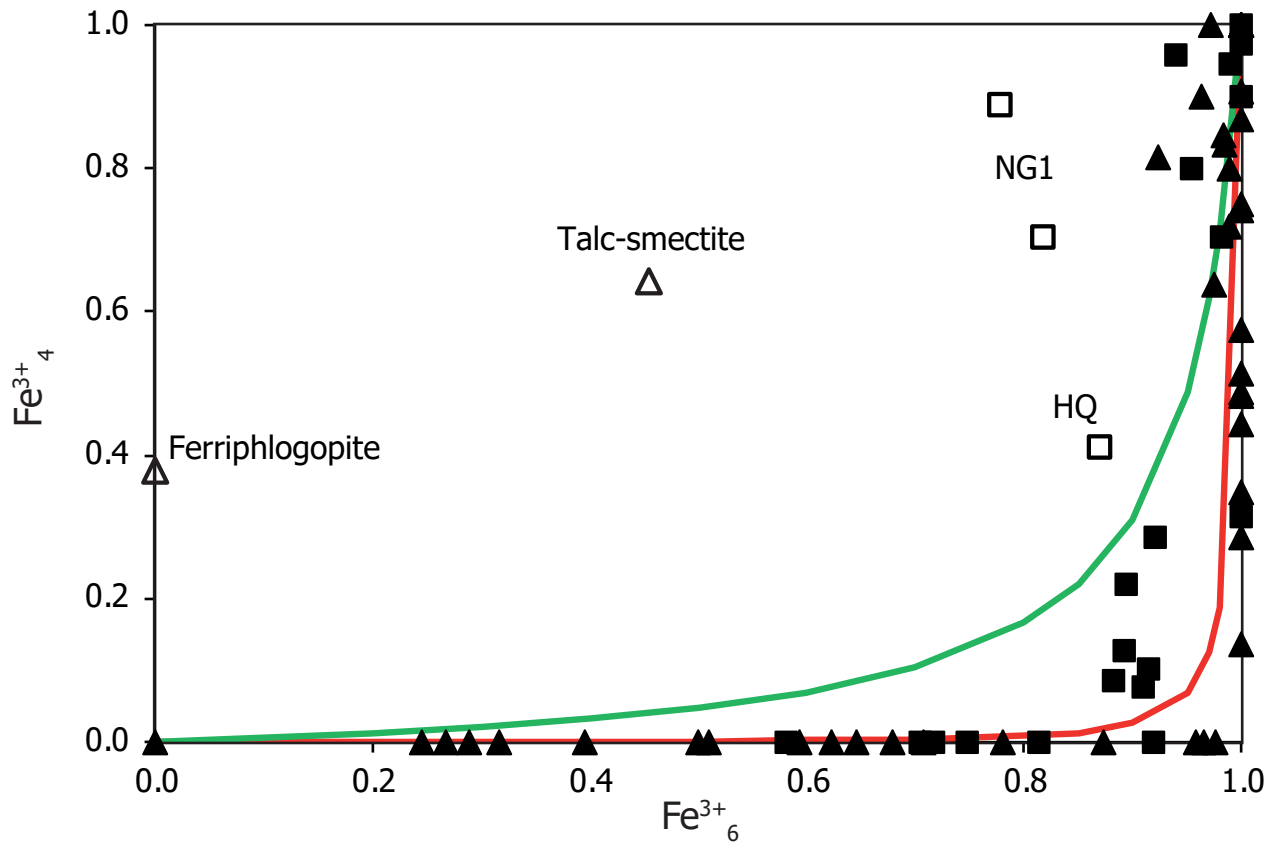


Figure 2

